

RESEARCH PAPER

HEAT TREATMENT EFFECT ON INTERFACE MICROSTRUCTURE AND HARDNESS OF A MEDIUM CARBON STEEL CLADDED BY AISI 316 STAINLESS STEEL

Andrea Di Schino^{1*}¹ Università degli Studi di Perugia, Dipartimento di Ingegneria, Perugia, Italy

*Corresponding author: andrea.dischino@unipg.it, Università degli Studi di Perugia, Dipartimento di Ingegneria, Via G. Duranti 93, 06125 Perugia, Italy

Received: 30.05.2020

Accepted: 30.07.2020

ABSTRACT

Aim of this paper is to analyze the interface properties of a austenitic stainless steel clad by carbon steel. The considered cladding process as performed by an external supplier was performed by submerged arc welding (SAW). A layer is created between stainless steel and carbon steel interface of the clad plate, caused by chemical element diffusion. High hardness local values were determined in the carbon steel at interface with stainless steel. Heat treatments were carried out aimed to remove such hardness peaks. Results show that a sub-critical heat treatments are not suitable to remove them. On the other hand, microstructure refinement as obtained by quenching and tempering (Q&T) heat treatment allowed a reduction of local steel hardenability with consequent interface hardness reduction.

Keywords: cladding; hardness; heat treatment

INTRODUCTION

Steel clad plates are widely used in several fields [1–3]: among them, carbon steel plates overlaid by nickel containing alloys (especially austenitic stainless steels) are one of the most commonly used material. In fact, they guarantee elevated tensile properties coupled with corrosion resistance, as a consequence of the presence of both carbon and stainless steel. As a matter of fact, due to their surface properties, stainless steels are applied in all fields facing challenging requirements of corrosion resistance [4,5]. It is known that they are widely used in automotive applications [6], as construction and building materials [7,8], in the energy sector [9–11], in aeronautical applications [12] and in food industry [13–15]. Recently many efforts have been carried out aimed to develop stainless steels suitable for 3D printing by selective laser melting [16]. However, their low yield strength does not favor their application as structural materials. Based on the above considerations it is clear that overlaying carbon steel plates by stainless steels properly faces with several engineering applications requiring high tensile properties together with resistance in corrosive environments. Since the cladding layer correspond to about 20% of the total plate thickness, in this family of materials Cr and Ni contents are reduced in comparison to stainless steel plates with a following estimated material cost reduction ranging 30–50% [17, 18]. The most common methods adopted to clad carbon steel plates by stainless steels or Ni alloys include explosion welding [19], roll bonding and welding overlay [20–22]. Focusing about welding overlay, it is worth to be mentioned that many welding methods are nowadays used: shielded metal arc welding (SMAW) [23], submerged arc welding (SAW) [24], tungsten inert gas welding (TIG) [25], CO₂ arc welding [26,27] and laser welding [28]. All these techniques were applied in order to clad Q235 carbon steel plates by AISI 304 stainless steel. It is anyway well known that also austenitic stainless steel could be attacked by corrosion phenomena [29] in severe aggressive environments. This is mainly due to chromium carbides precipitation at steel grain boundaries after material exposition at temperatures ranging 540–860°C. As a consequence of such precipitation, a local Cr content lowering is detected at grain boundaries: therefore the stainless steel loss its corrosion resistance. At same way, also clad plates will behave at the same way [30]. In such materials element diffusion at interface needs to be considered when evaluating the corrosion resistance. Many previous works reported that there is a diffusion width between the carbon steel and the welded overlay, making the stainless steel and carbon steel well bond together [31]. A large literature has been developed concerning, such aspect (e.g.[32]). Results showed that chemical element diffusion at the interface, appears is the main mechanism affecting the bonding of steel plate [33–34]. This mechanism is mainly affected by the overlaying conditions, which also a strong effect on microstructure at interface. Carbon and stainless steel interface is characterized by different microstructural features and properties determining the local mechanical characteristic of the clad plate. It is reported that following to

element diffusion process a 15 µm layer is formed at interface. Such layer is characterized by stable mechanical characteristics. It is also shown that microstructure is not affected by any grain growth process [35]. The sub surface mechanical properties gradually changes moving along the thickness direction [36]. As a consequence such transition layer is beneficial generating a stable bonding between the two metals. This also assures a good mechanical resistance transition along the thickness. Carburation in the stainless steel side has been found and decarburization in carbon steel is detected [37]. Many studies were carried out aimed to assess the corrosion behavior at the inner surface of ultra-supercritical boilers. Often a hardness peak is detected at stainless/carbon steel interface [38]: such peak needs to be carefully taken as low as possible for the possible deleterious effect they should exert in the material performance. Therefore, a specific heat-treatment is required in order to improve hardness values at metals interface [39–45].

Aim of this paper is to analyze the interface properties of a austenitic stainless steel clad by carbon steel. The effect of heat treatment is reported in terms of microstructure and hardness at interface.

EXPERIMENTAL

Carbon steel was plates sizing 400 mm x 400 x 15 mm were clad by an external supplier with AISI 316 L. Two welding passes have been performed. The steel was received in the Q&T condition. The two steels chemical composition is reported in Table 1.

Table 1 Chemical composition (mass, %)

Alloy	Cr	Ni	Mo	Mn	C	Fe
AISI 316 L	18	8	1	1.5	0.02	Balance
Steel A	0	0	0	1.0	0.20	Balance

The welding supplier declared plate manufacturing process parameters were: weld metal dilution of 40%, 7 kg/h deposition, a deposit efficiency of 95%. Main welding parameters were: welding current=500 A, arc voltage=30 V, travel speed= 2 mm/s, stick out=35 mm, overlap=9 mm, heat input max=5.3 kJ/mm, preheat temperature=150 °C. A medium-C steel (steel A) was chosen as a substrate. Longitudinal and transverse metallographic specimens, taken from plates have been prepared for metallographic examination. In particular, the bi-metals interface has been assessed by Light Microscopy (LM) and Scanning Electron Microscopy (SEM). The low-alloy steel has been etched by Nital 2%, whilst the microstructure of the AISI 316L weld overlay has been revealed by etching with 50% HNO₃+50% H₂O. Hardness through-thickness profiles have been measured (HV₁₀) using steps of 0.3 and 0.5 mm at various locations on longitudinal sections. Specimens have been machined from the clad plate and heat treated at a laboratory scale. The effect of final heat treatment conditions on

hardness and microstructure have been investigated performing some stress-relieving (SR) treatments on specimens machined from the clad plate. The original specimens have been also fully re-treated to simulate a Q&T treatment after cladding of as-rolled plates. The heat treated samples have been assessed for microstructure and hardness. The following cases have been considered:

Table 2 Heat treatment conditions

Material state	Tests	
	Hardness	Microstructure
Q&T+ cladding	√	√
SR at 640 °C	√	√
SR at 660 °C	√	√
Q&T (920 °C/ 670°C)	√	√
Q&T (980 °/670°C)	√	√
Q&T (1000 °C/670 °C)	√	√

RESULTS

Defects relating to the overlay welding process were not detected. The different welding passes are put in evidence. A first welding pass with 2.0-2.5 mm thickness is detected followed by a second one ranging 1.2-2.0 mm (Figure 1). The heat affected zone (HAZ) is easily recognized in steel A after etching (Figure 2). The coarse grained heat affected zone (CGHAZ) is detected between adjacent welding passes in proximity of the fusion line. A detail of the CGHAZ is reported in Figure 2. Steel A microstructure is that typical of Q&T medium-C steels (Figure 3). The dendritic structure of the weld overlay (second pass) is evident in Figure 4.

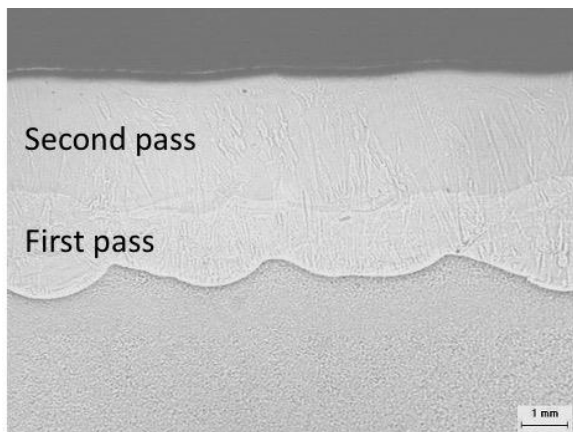


Fig. 1 Weld over-layed material (polished section)

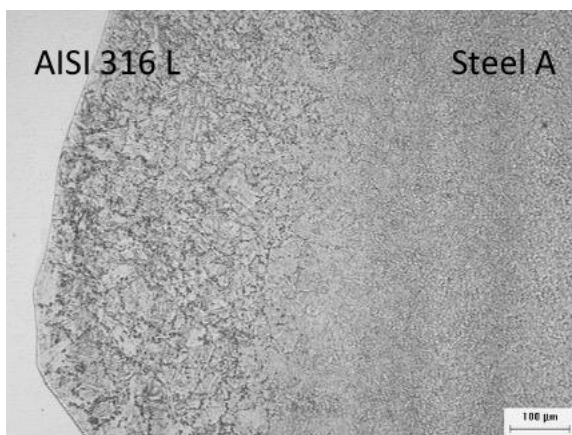


Fig. 2a Detail of CGHAZ (2% Nital etching) (LM image)

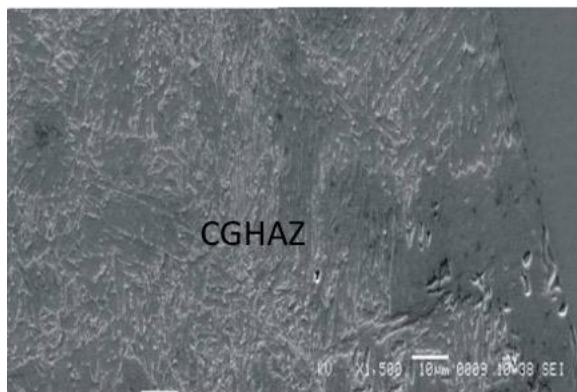


Fig. 2b Detail of CGHAZ (2% Nital etching) (SEM image)

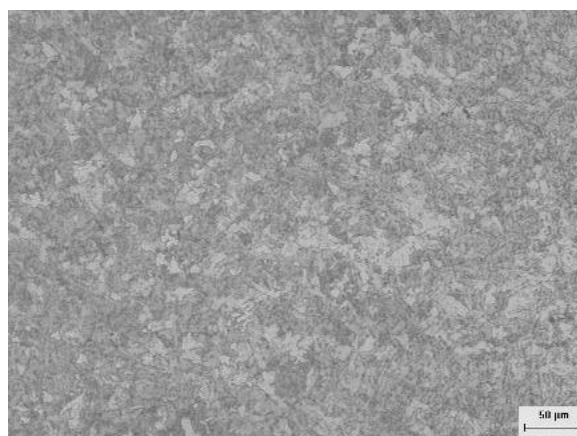


Fig. 3 Steel A substrate (Q&T material)

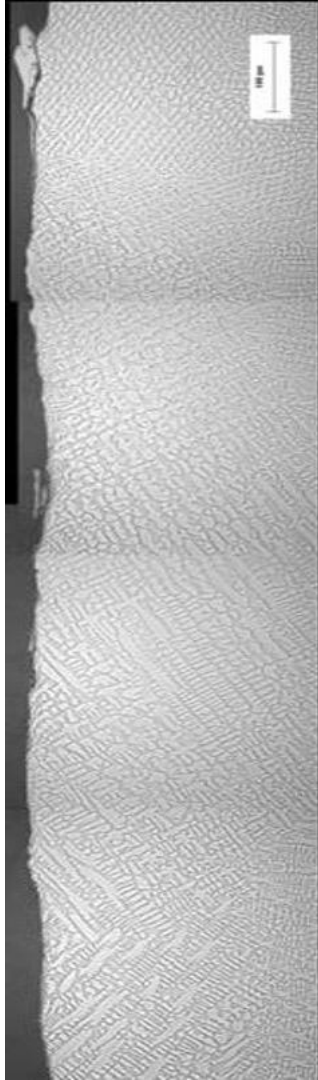


Fig. 4 AISI 316L cladding (etching: 50% HNO₃, 50% H₂O)

Examples of indentation array adopted to evaluate HV₁₀ hardness thickness profiles are reported in Figure 5. The hardness profiles (Figure 6) report hardness peaks (e.g. 250 to 270 HV₁₀) in steel A steel in proximity of the fusion line in the coarse grained heat affected zone.



Fig. 5 Interface indentation through thickness profiles

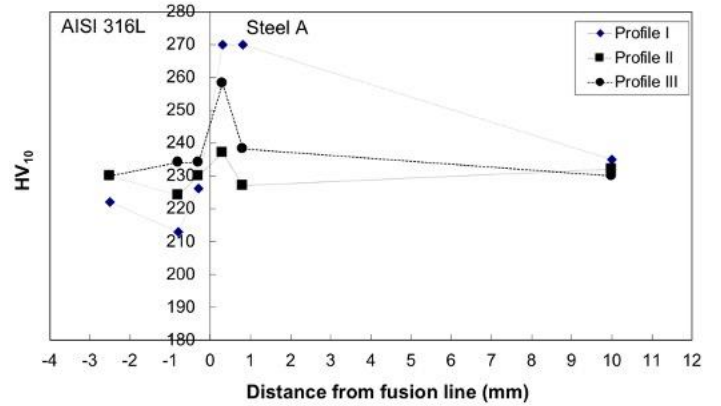


Fig. 6 Interface hardness profiles

Since such hardness peaks are not desired in such kind of products (brittle interface), different heat treatments (as reported in Table 2) were performed aimed to investigate their effect on interface hardness.

SR effect

Measured hardness profiles on the clad material after SR at 640 and 660 °C are reported in Figures 7 and 8. The hardness peaks in the coarse grain heat affected zone (e.g. 255 to 260 HV₁₀) are still present after SR, close to the fusion line even if a bit reduced in comparison to the as-received material. This means that SR is not effective to remove hardness peaks in the CGHAZ.

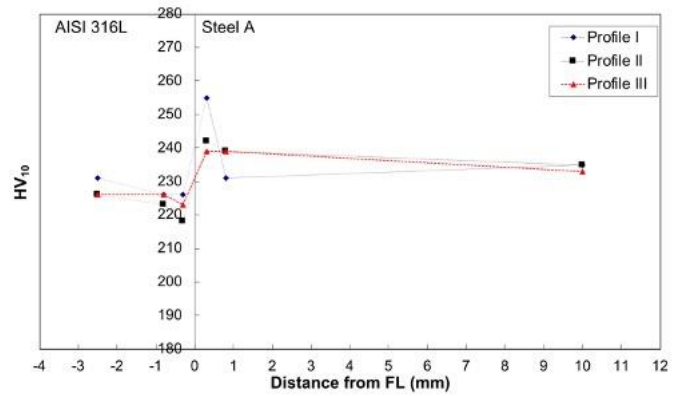


Fig. 7 Interface hardness profiles after SR@ 640 °C

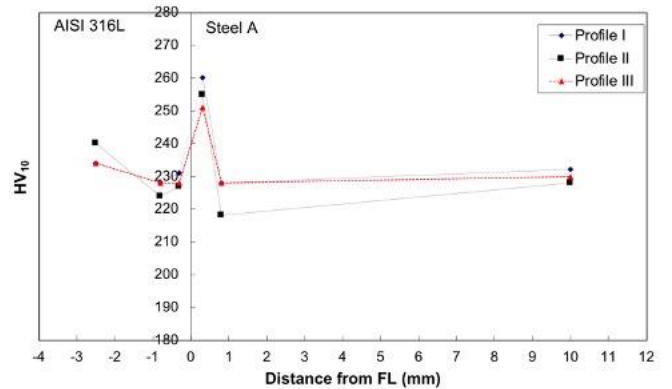


Fig. 8 Interface hardness profiles after SR@ 660 °C

Specimens were quenched and tempered: three different austenitizing temperatures (920 °C, 980 °C and 1000 °C) were exploited aimed to put in evidence the effect of prior austenite grain size; one tempering temperature (670°C) was analyzed, based on results from SR treatment effect, reporting about a poor sub-critical temperature effect. The austenitization temperatures were chosen aimed to reproduce the standard (unclad) medium-C plates austenitizzazione (920 °C), recommended annealing temperatures for AISI 316L stainless steel (980°C and 1000 °C). Such temperatures were also chosen since still practicable in furnaces during an industrial process. The measured hardness profiles on the clad material after quenching and tempering are reported in Figures 9.

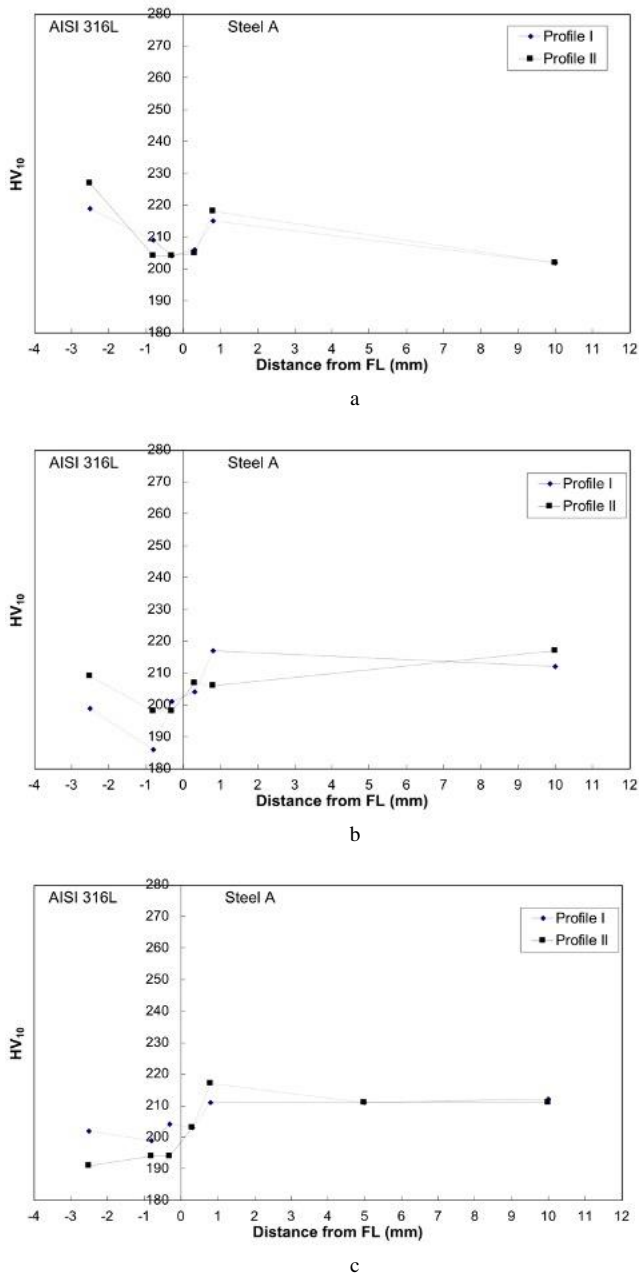


Fig. 9 Interface hardness profiles after Q&T at 920 °C/670 °C (a), 980 °C/670 °C (b) 1000 °C/670 °C (c)

The hardness peaks in the coarse grain heat affected zone of the carbon steel, close to the interface, disappeared: as a matter of fact all the measured values are

lower than 220 HV₁₀. Microstructures at interface, after quenching and tempering, show a austenite grain size refinement, if compared to as-received material (Figure 10). Such grain refinement reduces the local steel hardenability, thus favoring the formation of lower hardness microstructure.

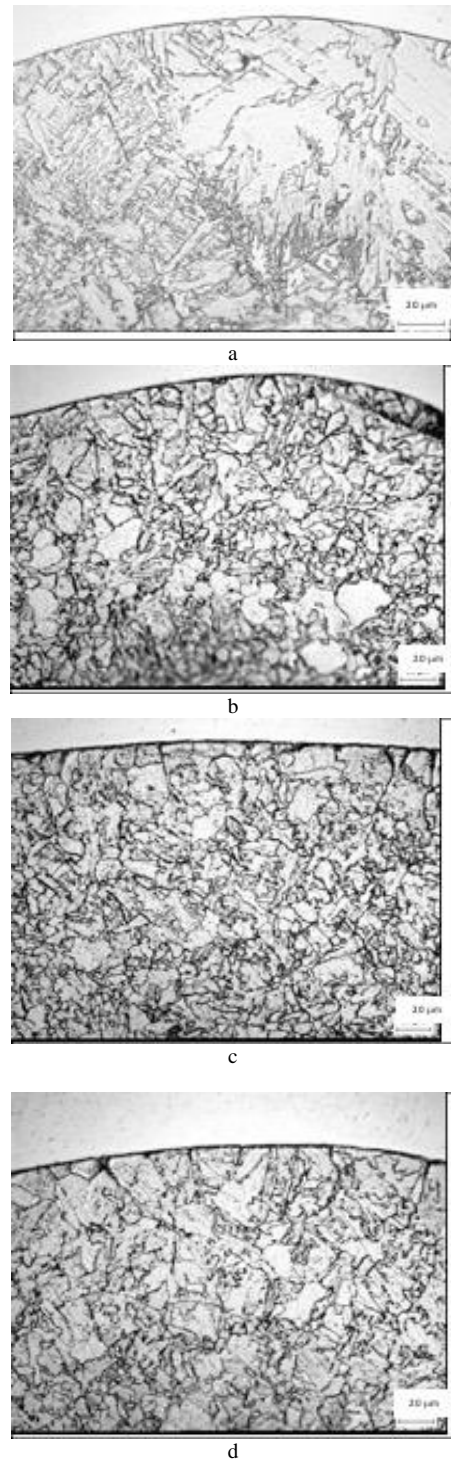


Fig. 10 Interface microstructure. a) as received material; b) 920 °C/670 °C; c) 980 °C/670 °C; d) 1000 °C/670 °C

The above result suggest that an alternative process route should be followed for manufacturing clad plates, consisting in the weld overlay of as-rolled plate, to be only subsequently quenched and tempered. The experienced temperature,

allowing the hardness peak reduction, as compatible to those of industrial Q&T processes.

CONCLUSIONS

From the results above reported it can be concluded that:

- Some hardness peaks (e.g. 250 to 270 HV₁₀) were revealed in the carbon steel near the fusion line in the coarse grained heat affected zone.
- The hardness peaks in the coarse grained heat affected zone of the carbon steel at 0.3 mm distance from interface, disappeared after quenching and tempering, being all values lower than 220 HV₁₀. This means that the re-austenitizing treatment, carried out at temperatures below those detected at 0.3 mm from interface, implies austenite grain size refining and that such effect promotes hardenability (hence hardness) reduction after tempering.
- This suggests that an alternative process route or manufacturing clad plates, consisting in the weld overlay of as-rolled plate, to be only subsequently quenched and tempered.

REFERENCES

1. K.S. Lee, D.H. Yoon, Kim, H.K., Y. N. Kwon, Y.S. Lee: Mater. Sci. Eng. A, 556, 2012, 319. <https://doi.org/10.1016/j.msea.2012.06.094>
2. C.Y. Liu, Q. Wang, Y.Z. Jia, R. Jing, B. Zhang, M.Z. Ma, R.P. Liu: Mater. Sci. Eng. A, 556, 2012, 1. <https://doi.org/10.1016/j.msea.2012.06.046>
3. S.U. Hang, X.B. Luo, F. Chai, J.C. Shen, X.J. Sun, F. Lu: J. Iron Steel Res. Int., 22, 2005, 977. [https://doi.org/10.1016/S1006-706X\(15\)30099-6](https://doi.org/10.1016/S1006-706X(15)30099-6)
4. P. Marshall: *Austenitic stainless steels: Microstructure and Mechanical Properties*. Springer, Netherlands, 1984.
5. A. Di Schino: Metals, 10, 2020, 327. <https://doi.org/10.3390/met10030327>
6. R. Rufini, O. Di Pietro, A. Di Schino: Metals, 8, 2018, 519. <https://doi.org/10.3390/met8070519>
7. A. Di Schino, P.E. Di Nunzio, G.L. Turconi: Mater. Sci. Forum, 558-559, 2007, 1435. <https://doi.org/10.4028/www.scientific.net/MSF.558-559.1435>
8. A. Di Schino, J.M. Kenny, G. Abbruzzese: J. Mater. Sci., 37, 2002, 5291. <https://doi.org/10.1023/A:1021068806598>
9. G. Napoli, A. Di Schino, M. Paura, T. Vela: Metalurgija, 57, 2018, 111.
10. A. Di Schino: Acta Metall. Slovaca, 22, 2016, 266. <http://dx.doi.org/10.12776/ams.v22i4.815>
11. D.K. Sharma, M. Filippini, A. Di Schino, F. Rossi, J. Castaldi: Metalurgija, 58, 2019, 347.
12. A. Gloria, R. Montanari, M. Richetta, A. Varone: Metals, 9, 2019, 662. <https://doi.org/10.3390/met9060662>
13. A. Di Schino, L. Valentini, J.M. Kenny, Y. Gerbig, I. Ahmed, H. Haefke: Surf. Coat. Technol. 161, 2002, 224. [https://doi.org/10.1016/S0257-8972\(02\)00557-1](https://doi.org/10.1016/S0257-8972(02)00557-1)
14. G. Bregliozzi, S.I. Ahmed, A. Di Schino, J.M. Kenny, H. Haefke: Tribol. Lett., 17, 2004, 697. <https://doi.org/10.1007/s11249-004-8075-z>
15. L. Valentini, A. Di Schino, J.M. Kenny, Y. Gerbig, H. Haefke: Wear, 253, 2002, 458. [https://doi.org/10.1016/S0043-1648\(02\)00140-0](https://doi.org/10.1016/S0043-1648(02)00140-0)
16. C. Zitelli, P. Folgarait, A. Di Schino: Metals, 9, 2019, 731. <https://doi.org/10.3390/met9070731>
17. A. Di Schino, P.E. Di Nunzio: Acta Metall. Slovaca, 23, 2017, 62. <https://doi.org/10.12776/ams.v23i1.852>
18. C. Li, G. Quin, Y. Tang, B. Zhang, S. Lin, P. Geng: J. Mater. Res. Tech., 9, 2020, 2522. <https://doi.org/10.1016/j.jmrt.2019.12.083>
19. Y. Wang, X. Li, X. Wang, H. Yan: Fusion Eng. Des., 137, 2018, 91. <https://doi.org/10.1016/j.fusengdes.2018.08.017>
20. Q. Qin, D. Zhang, Y. Zang, B. Guan: Adv. Mech. Eng., 7, 2015, 1. <https://doi.org/10.1177/1687814015594313>
21. Y. Li, H. Liu, Z. Wang: Mater. Sci. Eng. A, 731, 2018, 377. <https://doi.org/10.1016/j.msea.2018.06.039>
22. A. Mousawi, S. Barrett, S. Al-Hassani: J. Mater. Process. Technol., 202, 2008, 224. <https://doi.org/10.1016/j.jmatprotec.2007.09.028>
23. M. Tian, H. Chen, Y. Zhang, T. Wang, Z. Zhu: Heat Treat. Metal, 40, 2015, 110. <https://doi.org/10.13251/j.issn.0254-6051.2015.06.024>
24. T. Qiu, B. Wu, Q. Chen, W. Chen: Neiranji Gongcheng/Chinese Internal Combustion Engine Engineering, 34, 2013, 83.
25. H. Liao, K. Song, Y. Cao, M. Zeng: Hot Working Technol., 41, 2012, 148.
26. W. Wang, Y. Wang, M. Liu, F. Cheng, W. Wu: Hanjie Xuebao/Transactions of the China Welding Institution, 31(6), 2010, 89.
27. J. Zhang, Z. Ju: Steel Constr., 27, 2012, 48.
28. S. Missori, F. Murdolo, A. Sili: Weld J., 83(2), 2004, 65s.
29. J. Xin, Y. Song, J. Fang, J. Wei, C. Huang, S. Wang: Fusion Engineering and Design, 133, 2018, 70. <https://doi.org/10.1016/j.fusengdes.2018.05.078>
30. G. Aydogdu, M. Aydinol: Corr. Sci., 8, 2006, 3565. <https://doi.org/10.1016/j.corsci.2006.01.003>
31. H. Li, L. Zhang, B. Zhang, Q. Zhang: Materials, 12, 2019, 509. <https://doi.org/10.3390/ma12030509>
32. Z. Li, X. Wang, Y. Luo: Materials, 11, 2018, 2326. <https://doi.org/10.3390/ma11112326>
33. Y. Jing, Y. Qin, A. Zang, Q. Shang, H. Song: J. Alloys Compd., 617, 2014, 688. <https://doi.org/10.1016/j.jallcom.2014.07.186>
34. B. Liu, J. Wei, M. Yang, F. Yi, K. Xu: Vacuum, 154, 2018, 250. <https://doi.org/10.1016/j.vacuum.2018.05.022>
35. Z. Dhib, N. Guermazi, A. Ktari, M. Gasperini, N. Haddar: Mater. Sci. Eng. A, 696, 201, 374. <https://doi.org/10.1016/j.msea.2017.04.080>
36. T. Yu, A. Jing, X. Yan, W. Li, Q. Pang, G. Jing: J. Mater. Process. Technol., 266, 2019, 264. <https://doi.org/10.1016/j.jmatprotec.2018.06.007>
37. C.X. Chen, M. Liu, B. Liu, F. Yin, Y. Dong, X. Zhang, F. Zhang, Y. Zhang: Fusion Eng. Des., 125, 2017, 431. <https://doi.org/10.1016/j.fusengdes.2017.05.136>
38. S. Zhang, H. Xiao, X. Xie, L. Gu: J. Mater. Process. Technol., 214, 2014, 1205. <https://doi.org/10.1016/j.jmatprotec.2014.01.006>
39. A. Di Schino, L. Alleva, M. Guagnelli: Mater. Sci. Forum, 715-716, 2007, 860. <https://doi.org/10.4028/www.scientific.net/MSF.715-716.860>
40. H. Song, H. Shin, Y. Shin: Ocean Eng., 122, 2016, 278. <https://doi.org/10.1016/j.oceaneng.2016.06.042>
41. P. Petrousek, T. Kvackaj, R. Kocisko, J. Bidulska, M. Luptak, D. Manfredi, M.A. Grande, R. Bidulsky: Acta Metall. Slovaca, 25(4), 2019, 283. <http://dx.doi.org/10.12776/ams.v25i4.1366>
42. T. Kvackaj et al.: Journal of Materials Engineering and Performance, 29(3), 2020, 1509-1514. <https://doi.org/10.1007/s11665-020-04561-y>
43. R. Bidulsky, J. Bidulska, M. Actis Grande: Met. Sci. Heat Treat., 58(11-12), 2017, 734. <https://doi.org/10.1007/s11041-017-0087-z>
44. R. Bidulsky, M. Actis Grande, E. Dudrova, M. Kabatova, J. Bidulska: Powder Metall., 59(2), 2016, 121. <https://doi.org/10.1179/1743290115Y.0000000022>
45. R. Bidulsky, J. Bidulska, R. De Oro, E. Hryha, M. Maccarini, I. Forno, M. Actis Grande: Acta Physica Polonica A, 128(4), 2015, 647-650. <http://dx.doi.org/10.12693/APhysPolA.128.647>